A99-33772

AIAA 99–3438

Parallel Simulations of Turbulent Reacting Sprays

S. Menon W-W. Kim V. K. Chakravarthy S. Pannala and W. Henry
School of Aerospace Engineering
Georgia Institute of Technology
Atlanta, Georgia 30332

30th Plasmadynamics and Lasers Conference
28 June - July 1, 1999 / Norfolk, VA

Parallel Simulations of Turbulent Reacting Sprays

S. Menon* W-W. Kim† V. K. Chakravarthy‡ S. Pannala§ and W. Henry¶
School of Aerospace Engineering
Georgia Institute of Technology
Atlanta, Georgia 30332

A new parallel two-phase compressible 3-D flow solver has been developed to study high Reynolds number reacting flows. A key feature of this new solver is the manner in which small-scale turbulent mixing and combustion is simulated. This feature allows proper characterization of the effects of both large-scale convection and small-scale mixing on the scalar processes thereby, providing a more accurate prediction of chemical reaction effects. Since this methodology is new, a series of validation studies were first carried out using configurations such as the stagnation point and the bluff-body stabilized premixed flames for which data was available for comparison. The ability of the subgrid two-phase model is also demonstrated by simulating droplet vaporization (with infinite and finite-rate kinetics) in mixing layers. Finally, the LES solver is used to simulate high Reynolds number vaporizing liquid spray in a General Electric co-axial full-scale combustor. These spatially evolving 3D LES of fuel sprays is the first reported study for full-scale test conditions. Results show excellent agreement with data and provide confidence about the present LES approach. The unique nature of the methodology developed here also provides new insight into the physics of combustion process that was impossible using conventional approaches. The development of the two-phase LES has now established a simulation tool that can be used to study realistic spray flames in order to develop guidelines for the design of next generation advanced fuel injectors.

1 Introduction

Desirable features for the next generation gas turbine engines are combustion efficiency, reduced emissions and stable combustion in the lean limit. To reach these goals, current research is focusing on improving the liquid fuel atomization process and to increase fuel-air mixing downstream of the fuel injector. However, the structure of complex three-dimensional, swirling fuel-air mixing layers is very difficult to resolve using current experimental and numerical methods. Since fuel atomization and fuel-air mixing are both highly unsteady, conventional steady state methods cannot be used to elucidate the finer details. On the other hand, although unsteady mixing process can be studied quite accurately using direct numerical simulation (DNS),[1] application of DNS is limited to low to moderate Reynolds numbers (Re), typically of order 1000, due to resolution requirements. Here, an alternative approach using large-eddy simulation (LES) is being developed for high Re (order of 10,000 and more) flows.

In LES modeling of the momentum transport scales larger than the grid size are computed using a time- and space-accurate scheme, while the effect of the unresolved smaller scales (assumed to be mostly isotropic) on the resolved motion is modeled using an eddy viscosity based subgrid model. This approach is acceptable for momentum transport since all the energy containing scales are resolved and all the unresolved scales (that primarily provide for dissipation of the energy transferred from the large scales) can be modeled by using an eddy dissipation subgrid model. However, these arguments cannot be extended to reacting flows since, for combustion to occur, fuel and oxidizer species must first mix at the molecular level. Since, this process is dominated by the mixing process in the small-scales, ad hoc eddy diffusivity concepts cannot be used except under very specialized conditions. To deal with these distinctly different modeling requirements, a new subgrid mixing and combustion model has been developed that allows for proper resolution of the small-scale scalar mixing and combustion effects within the framework of a conventional LES approach. Validation of this method in reacting flows is demonstrated in this paper.

*Professor, AIAA Senior Member
†Post-Doctoral Fellow, AIAA Member
‡Graduate Research Assistant, AIAA Student Member
§Graduate Research Assistant, AIAA Student Member
¶Undergraduate Assistant, AIAA Student Member

The above noted subgrid methodology was originally developed for gas phase combustion. Here, we have extended this approach to deal with two-phase (primarily liquid-gas) flows with the goal of studying fuel spray combustion in high Reynolds number flows. In order to do this the LES formulation needs to be capable of capturing the physics of the two-phase mixing in an accurate manner.

The present two-phase LES approach employs the separated flow (SF) model which has been shown to be suited for spray modeling since it allows quantitative prediction of the effects of spray. However, SF models require accurate treatment of the finite rate exchange of mass, momentum and energy between the phases. Current models generally average over processes which occur on scales comparable to the drop size, i.e. no attempt is made to model the flow field around or within individual drops due to resource (CPU as well as storage) constraints. Usually these details are incorporated through empirical expressions for droplet drag, heat and mass transfer. The SF model can be further divided into three broad categories: discrete droplet (DD), continuous droplet (CD) and continuous formulation (CF) methods. Both DD and CF methods are commonly used to model two-phase flows and are also popularly referred as Lagrangian and Eulerian formulations for dispersed-phase, respectively. In the Eulerian formulation the motion of drops and gas are treated as though they are inter-penetrating continua. The resulting governing equations for both media are similar and very easy to model but it is very difficult to incorporate the effects of a range of droplet sizes. There are also several unresolved issues concerning the implementation of boundary conditions and coupling terms.[2] On the other hand, Lagrangian formulation explicitly tracks the droplets within the flow field and therefore, many intrinsic features of the droplets critical for accurate predictions can be included. Although both Eulerian and Lagrangian formulations have been used to simulate two-phase flows in the past,[3,4] most state-of-the-art codes employ the Lagrangian form (DD) to explicitly track the droplets while the gas phase is computed in the Eulerian form.[5] However, a key limitation of this approach is that due to resource constraints only a limited range of droplet sizes are tracked and droplets below an ad hoc (pre-specified) cut-off size are assumed to vaporize instantaneously and to become fully mixed in the gas phase.

In the present LES approach, the Lagrangian modeling approach is extended by including a subgrid Eulerian two-phase model in which the effect of droplets below the cutoff size is explicitly included. As shown, this approach removes the major shortcoming of the conventional DD approach.

2 Formulation of the LES Model

The conventional LES methodology captures the effect of the grid-resolved scales of motion using a highly accurate numerical scheme (the scheme employed here is fourth-order-accurate in space and second-order-accurate in time) and the effects of the unresolved scales on the resolved motion are included using eddy viscosity based subgrid model for the momentum transport. To handle the distinctly different physics of scalar mixing and chemical reactions a new subgrid model has been developed. Details of this model have been reported elsewhere[6-9] and therefore, only summarized here.

2.1 Subgrid Closure for Momentum Transport

The compressible LES equations are obtained by Favre-filtering Navier-Stokes equations using a top-hat filter (appropriate for finite-volume schemes). The filtering process results in terms in the resolved LES equations that require modeling. The final LES equations are avoided here for brevity since they are described elsewhere.[10,11] In general, the subgrid terms representing the subgrid stress tensor, the subgrid heat flux, the subgrid viscous work, the subgrid species mass flux, and the subgrid enthalpy flux all require modeling.

The subgrid stresses in the LES momentum equations are modeled using an eddy viscosity, which in turn, is modeled in terms of the LES filter width Δ and the subgrid kinetic energy K^{sgs}.[12] A transport model equation for the subgrid kinetic energy is solved along with the other LES equations.[10,13,14] The effects of subgrid turbulence on the flame structure (and propagation) can be quantified in terms of the subgrid kinetic energy[11,15] and thus, it is advantageous to use this type of LES model for reacting flows. Another distinct advantage of this approach is that this model does not assume equilibrium between subgrid kinetic energy production and dissipation (implicit in algebraic models) and thus, helps to attribute a relaxation time associated with the non-equilibrium in the subgrid scales. Presumably, due to this feature, the subgrid kinetic models and it's variants are, specifically, found to be superior[16] for modeling complex flows such as the bluff body wake flow of present interest.

A Stochastic Separated Flow (SSF) formulation[3,5] is used to track the droplets using Lagrangian equations of motion. The present formulation is limited to dilute sprays and the effects of static pressure gradient, virtual-mass, Basset force and external body-

forces are neglected here. However, the inclusion of these terms is not expected to change the current approach. The gas phase velocity field used in the particle equations of motion is obtained using both the filtered LES velocity field and the subgrid kinetic energy.[17,18] This approach includes the stochastic turbulent dispersion effect into the formulation (via the subgrid kinetic energy). Note that this effect cannot be included when an algebraic eddy viscosity (e.g., Smagorinsky type) is used.

2.2 Subgrid Closure for Premixed Combustion

Two different modeling approaches are adopted here for modeling premixed combustion. The first approach, called LES-LEM here after, is a method of multiple scales in which the large scales are modeled on the three-dimensional LES grid and the subgrid scales are assumed to be isotropic and are modeled using a stochastic mixing model called the linear eddy model.[19] The second approach is a more conventional approach in which the wrinkling of the flame surface by subgrid turbulence and the resulting increase in burning rate are modeled by a subgrid flame speed model.[15] The difference between the model flame speed and the laminar flame speed accounts for the effects of subgrid turbulence of the propagation rate of the flame surface.

The LES-LEM approach conducts one-dimensional stochastic simulations in each LES cell. A stochastic simulation is a representation of the local small-scale processes occurring in the LES cell at scales that cannot be resolved on the three-dimensional LES grid. Flame propagation at laminar flame speed, S_L, on each of the subgrid domain is simulated using the G equation:[20] $dG/dt = -S_L|\nabla G|$.

A finite volume scheme with a binary representation of G (0 and 1) is used to represent the reactant (G=1) and the burnt product (G=0) and the flame is considered an infinitely thin surface separating the reactant and the product. Within each LES cell the flame (if it exists) propagates at the local laminar flame speed S_L in the 1D LEM domain. The 1D LEM domain is further discretized into smaller cells (LEM cells) the size of which is chosen to ensure that the smallest eddy in the flow (e.g., the Kolmogorov eddy) is fully resolved. Each LEM cell represents an equal fraction of the LES cell volume and hence, the total volume represented in the subgrid simulation equals the volume of the LES cell it is contained in. More detail are discussed elsewhere[6-9] and are omitted here for brevity.

The effect of turbulent small scale mixing in each LES cell is modeled stochastically using a turbulent stirring process[6,21] on the 1D subgrid domain. The stirring process is an ensemble of stochastic volume rearrangement events that mimic the effects of turbulent subgrid eddies on the scalar field. The key feature of this process is that the length scale distribution and the associated frequency of stirring events are chosen to reflect the eddy size distribution in the inertial range of 3D turbulence. Thus, the effects of three-dimensional small-scale turbulent mixing[6] is captured even though the local subgrid domains are one-dimensional. Studies in the past have shown that this propagation-stirring model of premixed flames using the G equation captures the topological structure[22] and turbulent propagation rates[21] of realistic premixed flames.

The large scale advection (due to LES filtered velocity) of the scalar field is conducted using a Lagrangian volume transport method (similar to the volume-of-fluid type front tracking schemes) as detailed earlier.[7-9] In this method, the LEM cells are transported from one LES cell to a neighboring LES cell to account for the volume transport due to the velocity at the interface between the two LES cells. The ability of this method to capture the flame as a thin front on the LES grid is found to be the key reason why LES-LEM is able to simulate flamelet type burning, as shown below.

The conventional flame speed model is also based on the G equation approach. A scalar (G) field in a fluid that self-propagates at speed S_L is used to model the flame surface here. The G equation on Favre-LES filtering leads to the following equation.[7]

$$\frac{\partial(\bar{\rho}\tilde{G})}{\partial t}+\frac{\partial(\bar{\rho}\tilde{G}\tilde{u}_j)}{\partial x_j} = -\overline{\rho_o S_L^o|\nabla G|}-\frac{\partial}{\partial x_j}\left[\bar{\rho}(\widetilde{u_j G}-\tilde{u}_j\tilde{G})\right] \quad (1)$$

Here, ρ_o is the reference density and S_L^o is the laminar flame corresponding to this value of density. The source term in the above equation, which includes the effect of subgrid turbulence (wrinkling due to subgrid eddies) is modeled using a flame speed model derived using the RNG theory[15] as: $\overline{\rho_o S_L^o|\nabla G|} = \rho_o u_f|\nabla\tilde{G}|$. Here, u_f is given in terms of the subgrid kinetic energy and S_L. The second term on the right side of the above equation represents the unresolved transport (due to subgrid velocity field) and is customarily modeled using a gradient diffusion assumption.[23,24] In the current research, the local subgrid flame structure is assumed to resemble a freely propagating turbulent flame with intensity K^{sgs} and length scale Δ. This one-dimensional turbulent flame is assumed to be well described by the Bray-Moss-Libby theory.[25] The model for turbu-

lent diffusion in Favre-time averaged BML theory is extended here to close the subgrid G transport as: $\widetilde{u_j G} - \tilde{u}_j \tilde{G} = \tilde{G}(1-\tilde{G})[\tau S_L - 2u'^{sgs}]$. Here, τ is $T_p/T_o - 1$, where T_o and T_p are respectively, the reactant and product temperatures. The model presented here accounts for co-gradient and counter-gradient diffusion. This is considered a substantial improvement over the gradient diffusion models because the presence of counter-gradient diffusion is now well established in both experiments[26] and direct simulations.[27]

2.3 Subgrid Closure for Two-Phase Fuel-Mixing and Combustion

The subgrid closure discussed above was primarily developed for gas phase combustion. To deal with two-phase combustion in a similar manner additional models have to be incorporated. Earlier studies[17,18,28] have discussed a new methodology that takes into account the physics of spray transport and mixing. As noted earlier, in a typical LES formulation of two-phase mixing and combustion the droplets are tracked using the Lagrangian formulation only up to a pre-specified cut off size. Beyond this cut-off the droplets are assumed to instantaneously evaporate and mix with the oxidizer. Although this choice of the cutoff size is determined by computational constraints, the somewhat arbitrary choice can have serious impact on the accuracy of the predictions.

The present subgrid closure model accounts for the vaporization and mixing of the droplets smaller that the cutoff so as to obtain a more accurate estimate of the mixing process. Thus, droplets are tracked using the Lagrangian method on the LES grid as in conventional approaches. However, once the droplets have become smaller than the cutoff size (which is chosen primarily from computational constraints since the time step for integrating the Lagrangian equations of motion of small droplets is very small) a new subgrid Eulerian two-phase model is employed to incorporate the effect of vaporization and mixing of drops smaller that the cutoff size. The primary mixing model used here is identical to the LEM model developed earlier for gas phase combustion except that now the effect of the liquid phase change into gas is also included. Another key feature of this approach is that even though the Eulerian two-phase model cannot explicitly track the small drops the local vaporization rate is chosen from a droplet distribution below the cutoff size. It has been shown that this approach can capture the final stages of mixing in a more accurate and physically consistent manner. It has also been demonstrated that with this new subgrid closure the cutoff size choice in the Lagrangian algorithm to be less restrictive. As a result, a larger cutoff size can be chosen without sacrificing accuracy and even computational effort.

3 Parallel Numerical Implementation

The LES model described above has been implemented in two different codes: a zero Mach number approximation based Navier-Stokes solver that simulates flow without acoustic waves (i.e., incompressible flows) and a fully compressible solver. The incompressible solver is a non-staggered finite-difference solver which uses a fifth-order accurate scheme to discretize the convective terms and a fourth order scheme for the viscous term. The compressible solver is fourth-order accurate in space. Both schemes are second order in time. Details of these schemes are reported elsewhere. The key difference between these two codes is that the compressible code is parallelized and implemented using MPI libraries whereas the zero-M code is implemented only on SGI systems using SGI parallel options. The zero-M code is semi-implicit in time and since it does not resolve the acoustic waves, the effective time-step is much larger than the allowable explicit time-step of the compressible code. As a results, even on 16- or 32- processors on a SGI-2000, the zero-M code is quite effective.

The compressible code is highly scalable and achieves nearly linear scale up with increase in the number of processors.[11] It should be noted that for combustor flow simulations under realistic conditions, compressible flow must be modeled since the coupling between the acoustic waves and the vortical motion in the combustor plays a major role in the combustion process. Our present strategy has been to develop some of the basic algorithms using the zero-M code and then implement them in the compressible code. It is expected that most of the simulations planned for the next year will be carried out using the compressible code since realistic test conditions have to be simulated.

A typical compressible gas-phase LES using 500,000 points requires 2 GB of memory (using 1 scalar) and on a 128-processor CRAY T3E requires around 10000 single processor hours to obtain sufficient flow-through times for statistical analysis. When two-phase flow is to be simulated, the computational cost using around 100,000 droplets is around 45,000 single processor hours for 10-12 flow through times (typically needed to obtain data for statistical analysis). Note that 500,000 grid points is consid-

ered very coarse for accurate LES and in the future we plan to use around 2 million grid points. The computational cost will therefore, increase proportionally.

4 Results and Discussion

This section summarizes the results obtained in this study. We begin with the studies that were intended to demonstrate and validate the new subgrid combustion model developed for LES. The subgrid combustion model is evaluated in high Re premixed flame configurations and then applied to study fuel-air mixing in a two-phase mixing layer. Subsequently, the application of the two-phase LES model to spatially evolving swirling spray mixing is demonstrated.

4.1 Stagnation Point Premixed Flames

In this section we highlight the results of the simulations of stagnation point flames using both the conventional and the subgrid combustion model. We focus here on burning in a wrinkled flamelet regime. In this regime the internal flame structure is undisturbed and the reaction zone is a single connected domain. The flame oscillates only slightly about it's mean position. For these cases, the contribution of subgrid turbulence to burning (subgrid wrinkling) is minimal. Calculations were carried out using the zero-M code with a grid of 89x129x129 for the conventional case and a grid of 69x89x89 (with 100 LEM cells in each LES cell) for the LES-LEM case.

The front tracking ability of the LEM-LES method is demonstrated in figure 1 by comparison with the conventional LES prediction. As shown, LEM-LES captures the flame as a thin wrinkled front whereas the flame is captured over a broader zone by the flame speed model based conventional LES. The finite difference scheme in the conventional LES leads to smoother wrinkles whereas the stochastic nature of (flame) area creation mechanism (subgrid stirring) in LEM-LES leads to a more wrinkled structure.

In most practical combustion system due to various stages of mixing, combustion can occur in non-premixed, partially premixed and premixed regimes. Even within the premixed regime the flame structure can have very different characteristics; for example, the thin flamelet-type structure in relatively low u'/S_L regime changes to a more corrugated flamelet structure in high u'/S_L regime. In the latter regime wrinkling is more 3D and some pockets of reactants separate from the main reaction zone and exist in isolation surrounded by the products. The transition from wrinkled to corrugated flamelet type is evident in figure 2 clearly demonstrating that LES-LEM is capable of capturing flame structure in this wide region whereas conventional LES is unable to do so.

A more quantitative comparison of the superior ability of LES-LEM can be obtained by comparing the predictions with experimental data. The mean and the rms velocity profiles predicted by the LEM-LES and the conventional LES are compared to experimental data[29,30] in figures 5 and 4. As shown, the mean is predicted fairly well by both models but the prediction of turbulence is much better in case of LEM-LES. Across the flame, the density decreases significantly and this causes the flow to accelerate tremendously across the flame. This results in very high (flame normal) velocities on the product side (compared to the reactants side). The unsteady oscillations of the flame at any given point in the flame brush thus, causes very high intermittency which in turn leads to an increase in u'.

This physics is captured quite accurately by the LEM-LES method. In the conventional LES, the flame structure has a finite thickness which is determined by the numerics (grid, scheme, etc.) As a consequence, the flow acceleration (due to the density drop) is much more gradual than in the case of LES-LEM. This smoothening of the flow gradients reduces the flow intermittency and hence, the conventional approach does not produce the peak in u' at the flame brush as in the experiments and the LES-LEM simulation. This problem is also typical of LES that use finite-rate chemistry and transport equations for chemical species on the LES grid. Note that, the resolution of any real flame on a 3D grid is impossible using current computational resources. Thus, the flamelet-type burning may never be captured using conventional methods. On the other hand, the LEM-LES method appears to achieve this goal due to the combination of the features of the subgrid LEM and the front tracking scheme.

The ability of the new LES-LEM method to capture accurately premixed flame characteristics under a wide range of operating conditions has established a new simulation capability that has the potential of dealing with combustion in realistic full-scale devices. The simulations using a simple but quite representative flow problem such as the stagnation point flame has been quite rewarding in elucidating the finer details of the flame structure. Additional flame characteristics such as the effect of tangential strain rate, flame curvature and flame alignment on the flame speed and flame stability has been analyzed and discussed elsewhere[9] and therefore, avoided here for brevity.

4.2 Bluff Body Stabilized Flames

Another test configuration that was use to validate the LES-LEM method is the bluff body stabilized flame. The configuration shown in figure 5 is a triangular bluff body in a premixed mixture stream in a straight rectangular channel. The key feature of this configuration (when compared to the stagnation point flames) is the spatial (i.e., inflow-outflow) nature of the flow and thus represents very closely configurations seen in realistic devices. The cross section of the bluff body is an equilateral triangle of side H, of $0.04m$. Past experimental studies[31-33] were part of a research program aimed at understanding the physics of premixed flames in near-practical combustors and providing a data base for validation of combustion models. The data from these studies has since been used to test various turbulence/combustion modeling approaches.[16,34-37] Thus, the particular choice of this problem facilitates a direct comparison of the present method with previously adopted modeling approaches in addition to experiments.

Constant streamwise mean velocity, u_o, of $37m/s$ ($17m/s$ in the non-reacting case) with added 4% turbulence is prescribed at the inflow of the combustor. The inflow turbulence is made isotropic to mimic the flow generated across the honeycomb screen used at the entry of the combustor in experiments. The inflow is prescribed to be a perfectly premixed mixture of propane and air at an equivalence ratio, ϕ of 0.65. Temperatures of the unreacted mixture and fully burnt products are set to $600K$ and $1800K$ respectively.

Two reacting flow simulations and one non-reacting flow simulation are briefly discussed here.[8] Case 1 corresponds to the non-reacting flow simulation and is conducted on 97 x 49 x 33 grid. Cases 2 and 3, respectively, correspond to turbulent flame simulations with the LEM-LES and the flame speed model. Both these simulations are conducted using a 129 x 49 x 64 grid.

The instantaneous spanwise vorticity fields for the three cases are visualized in figure 6. Anti-symmetric von Karman vortices are clearly seen in the non-reacting flow field. In a test case where the no-slip boundary conditions at the wall is replaced with a slip boundary conditions, these von Karman vortices bounce off the walls and persist for a very long distance downstream of the bluff body. It can, therefore, be concluded that these vortices are very strong and not susceptible to turbulent decay. The frequency of vortex shedding is found to be 98 Hz in the LES which agrees favorably with 102 Hz measured in experiments.

The *rms* of axial and wall normal velocities in the near wake region (x = 0.348m), which are primarily determined by the strength of the vortex structures are shown in figure 7. It is seen that the predictions of present non-reacting LES match the experimental values reasonably well. There is a slight over prediction of axial intensity in both the current and the earlier LES conducted by Fureby which is probably due to inadequate grid resolution as noted earlier.[38]

As seen in figure 6, the instantaneous vorticity field in case 2 (LEM-LES) is symmetric across the centerline. This is a significant deviation from the anti-symmetric shedding seen in cold flows. The von Karman vortices are formed primarily due to the flow bending around a bluff body and the subsequent Kelvin-Helmholtz (K-H) instability downstream. At initial stages, the vortex structures could be formed at the same time on either sides of the centerline. These vortex structures are very strong and each tries to prevent the downstream propagation of the other (through Biot-Savart's induction). Given that the convective velocity is finite, the vortex structures could eventually stop propagating. Such a state would be highly unstable and the flow in fact never reaches that state. Instead, a stable state of alternate vortex shedding is reached.

In the presence of chemical reactions, the vortex structures (formed due to the instability) try to entrain (wrap) the flame surface. When the chemical reactions are exothermic, the heat release due to the entrained flame sheet creates baroclinic torque that hinders the roll up of the shear layer[39] and reduces the vorticity magnitude drastically. Obviously, the baroclinic torque is a function of the density stratification due to the chemical reactions. If the density gradients are high, the baroclinic torque weakens the K-H instability and the vorticity magnitude is greatly reduced. When the density gradients are not very high, the K-H instability could still be strong enough to lead to an anti-symmetric vorticity structure and as a result, anti-symmetric flapping of the flame. This clearly explains the nature of the vorticity structure in case 3 and the earlier LES.[35]

The flame profile is resolved over a finite width in the LES with the flame speed model (case3). This is due to the fact that finite difference or finite volume schemes are incapable of capturing thin reaction fronts. In the G equation approach, the reaction zone is required to be infinitely thin or as thin as possible on the grid. In most combustors, the actual flame thickness is also very small. Even when a finite rate modeling approach[35] is used for combustion, the reaction zone is, in general, not accurately resolved.[40] have investigated the effects of numerical

flame thickness of the propagation characteristics of the flame and the reader is referred to their work for further discussion. The lack of fine resolution leads to flame thicknesses that are dictated by the numerics of the modeling approach. In the present conventional LES (case 3), the density gradients are lowered as a consequence of a thick flame. So the baroclinic torque generated is not very strong. The LES simulations conducted[36] using a reactant to product density ratio of 6.0 also do not show any anti-symmetric flow structure. In this case, the density gradient are higher than in the case of density ratio of 3.0[35] only because of the higher density difference. This deviation from anti-symmetric flow structure with increasing density gradients (stratification) is consistent with the arguments presented here.

The symmetric structure of the flame in the near wake region, as predicted by LEM-LES, is quite common in bluff body stabilized wakes.[36,41] The possible cause of this will be discussed further in the future. As seen in figure 6, the large scale vortices interact with turbulence to create small scale disturbances which in turn wrinkle the flame surface and enhanced propagation. This is once again due to the fact that a thin flame is more susceptible to the local flow disturbances than thick flames.[40] In contrast to case 2, large scale (and anti-symmetric) flapping of the flame is observed in case 3 and previous LES approaches. Also, no significant small scale wrinkling is seen downstream.

The *rms* of axial and wall normal velocities in the near wake region (x = 0.348m), which are primarily determined by the strength of the vortex structures are shown in figure 7. It is seen that the predictions of present non-reacting LES match the experimental values reasonably well. There is a slight over prediction of axial intensity in both the current and the earlier LES conducted by Fureby which is probably due to inadequate grid resolution as noted earlier.[38] Also shown for comparison is the prediction using monotonically integrated LES (MILES) obtained using a much higher resolution grid of 400x60x60.[42]

The intensity of velocity fluctuations at the first location for the reacting cases are presented in fig 8. Significant peaks are noticeable in the measured velocity fluctuations. The peaks could be due to the passage of vortex structures (symmetric or anti-symmetric as the case may be) or the flapping of the flame surface. The flapping of the flame across which the normal velocity is magnified could lead to an increased intermittency of the flame normal velocity.[26] Since the flame flapping is predominantly in the vertical (wall normal) direction, the peaks in v' are, at least in part, due to flame oscillations. This argument is further strengthened by the fact that v' profile at the same location does not have twin peaks in the non-reacting flow.

Only the LES with a flame-speed model produces the twin peaks in axial intensity though a weak tendency of LES-LEM to produce these peaks is noticeable. Given that the thin reaction zones are better captured by the LES-LEM approach, it is surprising that a more conventional flame speed model predicts more noticeable peaks like in experiments. This is a mere coincidence which can be explained as follows. By comparing fig 8 with figure 7 (the corresponding cold flow results), it is seen that the intensity of velocity fluctuations in the flame speed model simulations are very close to those predicted in the non-reacting case. So the twin peaks in u' for this reacting case are produced by the passing of the anti-symmetric vortex structures rather than due to flame oscillations. The maximum anisotropy ($= v'/u'$) in the wake was found to be 1.3[31] where as the conventional model predicts a value of 2.5 which is very similar to the non-reacting case. LEM-LES produces a maximum anisotropy of 0.9 which is lower than in the experiments due to over prediction of u' on the centerline. This over-prediction is perhaps related to the poor resolution like in the non-reacting case. The tendency for u' peak formation is slightly evident in LES-LEM and perhaps stronger more resolved peaks would emerge if better resolution is used in zones where the flame flapping occurs (zone of density gradients). The anti-symmetric flame oscillations in the LES conducted by Fureby entrain the reactants deeper into the wake region. There is more possibility of finding reactants on the center-line in such a simulation. The velocity intermittency due to this intermittent presence of reactants among products could be the reason for the peak produced at the wake centerline by the eddy dissipation model.

4.3 Droplet vaporization in Mixing Layers

The subgrid combustion model developed above was extended to deal with two-phase mixing in an earlier study.[17,18] Figure 9 shows the product density in a temporal mixing layer as predicted by conventional LES and the new subgrid based LES. As shown, when the cutoff size is increased, the conventional LES predicts widely different product formation. However, this is an error since the amount of fuel present is the same and the choice of the cutoff size should not affect the prediction of the product formation. The failure of the conventional LES is due to its implicit assumption that all droplets

smaller than the cutoff size instantaneously vaporize and mix with the oxidizer. Thus, as the cutoff size increases, the conventional LES assumes more liquid is instantaneously evaporating and as a result more product formation is predicted.

On the other hand, the new subgrid two-phase model does not make this assumption. In fact, it assumes that the droplets below the cutoff size continue to vaporize at a rate determined by the droplet size distribution within the subgrid. Thus, the mixing process continues unabated till all drops (accounted in the subgrid as a void fraction in the Eulerian two-phase approach) have been vaporized. The new methodology deals with the final stages of mixing in an accurate manner thereby predicting product formation that is relatively independent of the chosen cutoff size. This is clearly seen in the figure where is shows that increasing the cutoff size does not impact the final product formation significantly.

There is another advantage of the new subgrid based mixing model. As is well known, as the cutoff size decreases, the time step to evolve the droplet equations decreases and the computational cost increases substantially. Thus, increasing the cutoff size (which is not possible in conventional LES due to large errors) decreases the overall cost of the LES. This was observed in recent simulations where it was noted that increasing the cutoff size by a factor of four decreased the computational cost by nearly a same factor in-spite of the increased computational effort needed to simulate the subgrid mixing process in the LES-LEM approach. This improved efficiency of the LES-LEM without sacrificing accuracy is an unique feature of the present model that provides some confidence that the LES-LEM approach can be used for practical spray combustion without exceedingly increasing the computational cost.

4.4 Spatially evolving turbulent sprays

The LES model developed here is now at a stage where it can be used to study flows of more practical interest. Of particular focus here is the study of liquid spray evolution (even when chemical kinetics are neglected) in a highly swirling turbulent flow. In the current study, spray in a highly swirling spatially evolving flow is analyzed for the interaction between the gas-phase and the dispersed phase. Three different cases were simulated and analyzed: a) No coupling between the gas-phase and the dispersed phase, b) Momentum coupled and c) Momentum and Vaporization coupled with infinite rate chemistry with no heat release. All simulations were carried out using a grid resolution of 101x61x81 and approximately 65,000 particles. A typical simulation using the compressible code required around 40000 single processor Cray T3E hours for around 10 flow through times.

The mass flow corresponding to a mass fraction (mass of gas-phase to that of liquid-phase) is approximately 0.1 since the present formulation is limited to dilute sprays. A log-normal distribution was used to chose the size of the droplets. Only the case with full coupling with vaporization and infinite rate kinetics is discussed below.

Figure 10 shows an instantaneous 3D view of the swirling flow in the combustor. The circular plane in the axial direction shows the vorticity magnitude and the spanwise plane shows the product density formed when the vaporized fuel reacts with the oxidizer. As can be noted the swirling incoming jet expands rapidly. The unsteadiness and high levels of turbulence intensities in the swirling shear layer can be seen in these figures. Flow visualization indicates that there is a complex pattern of vortex shedding in addition to vortex stretching associated with swirl. However, most of these details are lost when time averaging of the data is carried out (not shown here). This loss of information even when LES data is time-averaged shows clearly the need to analyze the time-evolving data obtained during the simulation in order to obtain a deeper insight into the flow and mixing processes.

Figure 11 show a typical instantaneous center plane view of the vorticity magnitude and the corresponding droplet distribution. As shown the high swirl in the incoming flow rapidly spreads out the shear layer and the shear layer breaks up into highly stretched vortical structures. The droplet spray is also significantly affected by the flow swirl. This effect when combined with the initial spray cone direction rapidly transports the droplets in the whole region. Smaller drops get transported further out; however, note the present calculation includes the formation of product when the droplets vaporizes and the gaseous fuel reacts with the oxidizer. Therefore, the distribution shown here includes the effect of vaporization.

Figures 12 and 13 show respectively, the droplet and the product density distributions at $x/D = 1.13$ at two instants in time. At this location significant product formation occurs. Significant effect of swirl is apparent in these figures. Analysis shows that the product is formed in regions in-between large concentration of droplets. Comparing with the vorticity distribution shows that droplets tend to collect in regions of low vorticity typically around the periphery of the vortex structures. Additional data in terms

of droplet size distribution and turbulent correlation has been obtained and is being analyzed. These results will be reported in the near future.

5 Conclusions

The results reported here for premixed combustion under experimentally studied conditions demonstrate that resolution of the flame plays a key role in determining flame-turbulence interactions in LES. The subgrid propagation simulated in LEM, along with the front tracking scheme used in LES-LEM, is found to be fairly accurate in capturing key features of flamelet combustion.

The study of the bluff-body stabilized flames has shown that the LES-LEM approach is capable of capturing flamelet combustion more accurately than other well established approaches. The LES-LEM predicts a flame structure that is closer to the experiments, *i.e.* breakdown of a smooth flame sheet in the near wake region into a highly wrinkled flame surface downstream. Due to the anti-symmetric flame flapping in the flame speed simulation here and the past simulations, the cold reactants are entrained better into the core region (centerline) of the wake. In earlier approaches based on diffusion-reaction models for the flame,[35,37] the flame is considerably thicker than in the present cases. The thin flame in the current flame speed simulation, while flapping in the vertical direction, leads to higher velocity intermittency (v') than in the conventional simulations. LES with a flame-speed model using a MILES approach[43] was found to produce results significantly different compared to the current flame speed simulation.

The present LES-LEM approach can be extended to finite-rate multi-species combustion chemistry (a goal of the present study). However, the present study suggests that the resolution of the flame structure along with an accurate estimate of subgrid reaction rates is essential for modeling premixed flames in any type of LES. This requirement has obvious implications regarding the computational capability needed for such simulations. Preliminary estimates suggest that for full 3D premixed (or non-premixed) combustion with relatively detailed finite-rate chemistry (e.g., 20 species) would require at least 512 processors with CPU speed at least 2-3 orders of magnitude faster than the current Cray T3E in order to complete a typical simulation in matter of days (provided the system is available for such a simulation). Although this requirement may look exorbitant, note that with the rapid increase in processor power, such simulations may become a reality within couple of years.

A two-phase compressible 3-D flow solver has also been developed and used to simulate droplets in a highly swirling co-axial full-scale combustor. In order to isolate the effects of the two-way interaction between the droplets and the gas phase, both coupled and uncoupled cases have been simulated. It has been found that the large scale recirculation zones of the combustor greatly effect the droplet distribution. Many of the computed features in the two-phase shear layer are in qualitative agreement with data. Comparison of the instantaneous flow features with the time-averaged features clearly show the need to use the unsteady data for analysis since significant details of the mixing process is lost when time-averaging is employed. These results also emphasize the need for LES type of approach to accurately study complex flows of practical interest.

A major problem facing two-phase LES development is the lack of detailed data for model validation. Recently data has become available from NIST for spray combustion that appears suitable for such a validation study. This effort is currently underway and results will be reported in the near future. Once the two-phase LES code is validated, simulations can address issues of related to design of advanced fuel injectors.

Acknowledgments

This work was supported by the Army Research Office under the Multidisciplinary University Research Initiative. Computational time was provided by DOD High Performance Computing Centers at NAVO, MS and SMDC, AL under a DOD Grand Challenge Project.

References

[1] Poinsot, T., "Using direct numerical simulations to understand premixed turbulent combustion," *Symp. (Intn.) on Combustion*, Vol. 26, 1996, pp. 219–232.

[2] Crowe, C., Sommerfeld, M., and Tsuji, Y., CRC Press, 1996.

[3] Faeth, G. M., "Evaporation and combustion of sprays," *Progress in Energy and Combustion Science*, Vol. 9, 1983, pp. 1–76.

[4] Mostafa, A. A. and Mongia, H. C., "On the modeling of turbulent evaporating sprays: eulerian versus lagrangian approach," *Int. J. of Heat Mass Transfer*, Vol. 30, 1983, pp. 2583–2593.

[5] Oefelein, J. C. and Yang, V., "Analysis of transcritical spray phenomena in turbulent mixing layers," *AIAA 96-0085, 34th AIAA Aerospace Sciences Meeting*, 1996.

[6] Menon, S., McMurtry, P., and Kerstein, A., "A linear eddy mixing model for LES of turbulent combustion," *LES of Complex Engineering and Geophysical flows*, edited by B. Galerpin and S. Orszag, Cambridge Univ. Press, 1993, pp. 287–314.

[7] Smith, T. and Menon, S., "Subgrid combustion modeling for premixed turbulent reacting flows," *AIAA-98-0242*, 1998.

[8] Chakravarthy, V. and Menon, S., "Large-Eddy simulations of bluff body stabilized flames," *Proceedings of FEDSM'99 3rd ASME/JSME Joint Fluids Engineering conference*, 1999.

[9] Chakravarthy, V. and Menon, S., "Modeling of turbulent premixed flames in the flamelet regime," *Proceedings of first International Symposium on Turbulent and Shear Flow Phenomena*, 1999.

[10] Kim, W.-W. and Menon, S., "A new incompressible solver for large-eddy simulations," *International Journal of Numerical Fluid Mechanics*, Vol. to appear, 1999a.

[11] Kim, W.-W. and Menon, S., "Large eddy simulation of a gas turbine combustor flow," *Combustion Science and Technology (to appear)*, 1999b.

[12] Schumann, U., "Subgrid scale model for finite difference simulations of turbulent lows in plane channels and annuli," *Journal of Computational Physics*, Vol. 18, 1975, pp. 376–404.

[13] Kim, W.-W. and Menon, S., "A new dynamic one-equation subgrid-scale model to turbulent wall-bounded flows," *AIAA 95-0356, 33rd AIAA Aerospace Sciences Meeting*, 1995.

[14] Menon, S. and Kim, W.-W., "High Reynolds number flow simulations using the localized dynamic subgrid-scale model," *AIAA 96-0425, 34th AIAA Aerospace Sciences Meeting*, 1996.

[15] Yakhot, V., "Propagation velocity of premixed turbulent flames," *Combustion Science and Technology*, Vol. 60, 1988, pp. 191–214.

[16] Fureby, C., "Towards large eddy simulations of flows in complex geometries," *AIAA-98-2806*, 1998.

[17] Menon, S. and Pannala, S., "Subgrid modeling of unsteady two-phase turbulent flows," *AIAA Paper No. 97-3113*, 1997.

[18] Pannala, S. and Menon, S., "Large eddy simulations of two-phase turbulent flows," *AIAA 98-0163, 36th AIAA Aerospace Sciences Meeting*, 1998.

[19] Kerstein, A., "Linear-eddy modelling of turbulent transport. Part 6. Microstructure of diffusive scalar mixing fields," *Journal of Fluid Mechanics*, Vol. 231, 1991, pp. 361–394.

[20] Kerstein, A. R., "Linear-eddy model of turbulent scalar transport and mixing," *Combustion Science and Technology*, Vol. 60, 1988, pp. 391–421.

[21] Smith, T. and Menon, S., "One-dimensional simulations of freely propagating turbulent premixed flames," *Combustion Science and Technology*, Vol. 128, 1996, pp. 99–130.

[22] Menon, S. and Kerstein, A., "A computational model to predict the fractal nature of turbulent premixed flames," *AIAA-94-0678*, 1994.

[23] Ashurst, W., Kerstein, Kerr, R., A.R., and Gibson, C., "Alignment of vorticity and scalar gradient with strain rate in simulated Navier Stokes turbulence," *The Physics of Fluids*, Vol. 30, No. 8, 1987, pp. 2343–2353.

[24] Im, H. G., Lund, T. S., and Ferziger, J. H., "Large eddy simulation of turbulent front propagation with dynamic subgrid models," *The Physics of Fluids*, Vol. 9, No. 12, 1997, pp. 3826–3833.

[25] Bray, K., Libby, P., and Moss, J., "Flamelet crossing frequencies and mean reaction rates in premixed turbulent combustion," *Combustion Science and Technology*, Vol. 41, 1984, pp. 143–172.

[26] Cho, P., Law, C. K., Cheng, R. K., and Shepherd, I. G., "Velocity and scalar fields of a turbulent premixed flame in a stagnation flow," *Twenty-second International Symposium (International) on Combustion*, 1988, pp. 739–745.

[27] Veynante, D., Trouve, A., Bray, K., and Mantel, T., "Gradient and counter gradient scalar transport in turbulent premixed flames," *Journal of Fluid Mechanics*, Vol. 332, 1997, pp. 263–293.

[28] Menon, S. and Pannala, S., "Subgrid combustion simulations of reacting two-phase shear layers," *AIAA Paper No. 98-3318 ,34th AIAA/ASME/SAE/ASEE Joint Propulsion Conference and Exhibit*, 1998.

[29] Cho, P., Law, C. K., Hertzberg, J. R., and Cheng, R. K., "Structure and propagation of turbulent premixed flame stabilized in a stagnation flow," *Twenty-first International Symposium (International) on Combustion*, Vol. 21, 1986, pp. 1493–1499.

[30] Cheng, R. and Shepherd, I., "A comparison of the velocity and scalar spectra in premixed turbulent flames," *Combustion and Flame*, Vol. 78, 1989, pp. 205–221.

[31] Sjunnesson, A., Nelson, C., and Max, E., "LDA measurements of velocities and turbulence in a bluff body stabilized flame," Tech. Rep. S-461 81, VOLVO Flygmotor AB, Trollhattan, Sweden, 1991.

[32] Sjunnesson, A., Olovsson, S., and Sjoblom, B., "Validation Rig - A tool for flame studies," Tech. Rep. 9370-308, VOLVO Flygmotor AB, Trollhattan, Sweden, 1991.

[33] Sjunnesson, A., Henriksson, P., and Lofstrom, C., "CARS measurements and visualization of reacting flows in bluff body stabilized flame," *AIAA-92-3650*, 1992.

[34] Ryden, R., Eriksson, L., and Olovsson, S., "Large eddy simulation of bluff body stabilised turbulent premixed flames," *International Gas Turbine and Aeroengine Congress and Exposition*, ASME 93-GT-157, New York NY, 1993.

[35] Fureby, C. and Lofstrom, C., "Large eddy simulations of bluff body stabilized flames," *Twenty-fifth International Symposium (International) on Combustion*, 1994, pp. 1257–1264.

[36] Moller, S. I., Lundgren, E., and Fureby, C., "Large eddy simulation of unsteady combustion," *Twenty-sixth International Symposium (International) on Combustion*, 1996, pp. 241–248.

[37] Inage, S., Perez, V., and Kobayashi, N., "An evaluation of premixed combustion around a bluff body using a combustion model," *JSME International Journal, Series B*, Vol. 41, No. 3, 1998, pp. 650–656.

[38] Akselvoll, K. and Moin, P., "Large-eddy simulation of turbulent confined coannular jets," *J. of Fluid Mech.*, Vol. 315, 1996, pp. 387–411.

[39] McMurtry, P., Jou, W.-H., Riley, J., and Metcalfe, R., "Direct numerical simulations of a reacting mixing layer with chemical heat release," *AIAA-85-0143*, 1985.

[40] McLaughlin, R. M. and Zhu, J., "The effect of finite front propagation on the enhanced speed of propagation," *Combustion Science and Technology*, Vol. 129, 1997, pp. 89–112.

[41] Veynante, D., Piana, J., Duclos, J. M., and Martel, C., "Experimental analysis of flame surface density models for premixed turbulent combustion," *Twenty-sixth International Symposium (International) on Combustion*, 1996, pp. 413–420.

[42] Fureby, C., "Large eddy simulations of anisochoric flows," *AIAA J.*, Vol. 33, 1995, pp. 1263–1272.

[43] Fureby, C., *On modeling of unsteady combustion utilizing continuum mechanical mixture theories and large eddy simulations*, Ph.D. thesis, Lund Institute of Technology, Lund, Sweden, 1995.

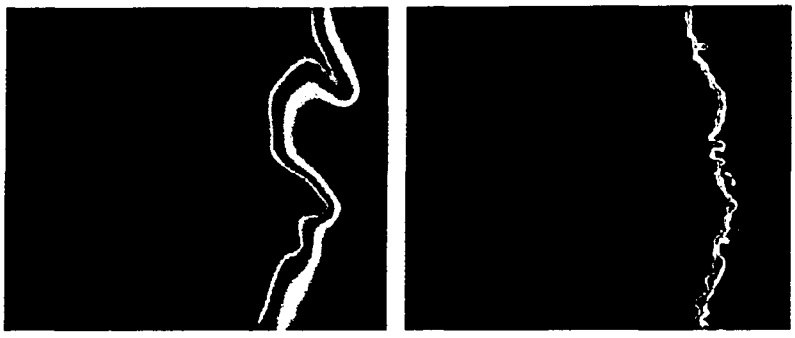

a) case1 : LES using a conventional flame model

b) case2 : LES using the new LES-LEM model

Fig. 1 Comparison of conventional LES and LES-LEM predictions in the flamelet regime as predicted in the stagnation point flow. As shown, LES-LES captures the flame as a thin wrinkled flame whereas the conventional LES numerically diffuses the flame.

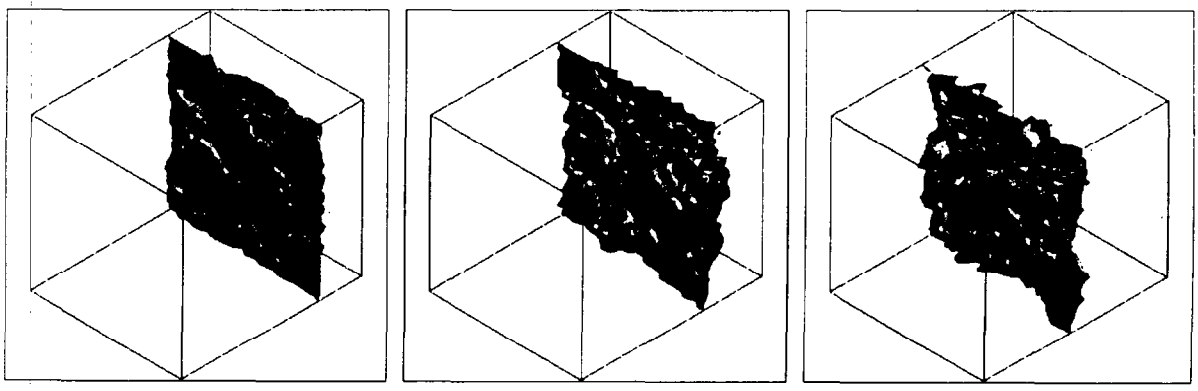

a) case1 : $u'/S_L = 1.5$ b) case1 : $u'/S_L = 4$ c) case1 : $u'/S_L = 8$

Fig. 2 Transition of the flame structure from the wrinkled flamelet type of burning to the corrugated type of burning with increasing u'/S_L as predicted by LES-LES.

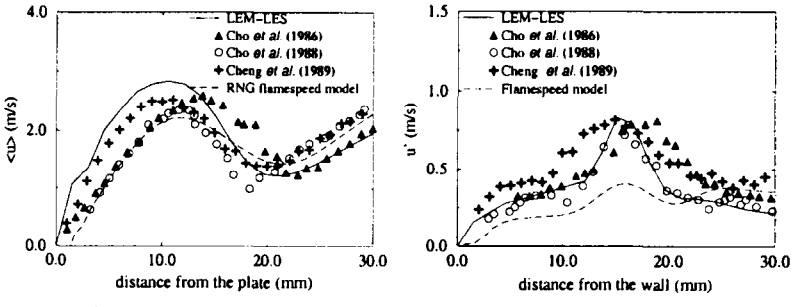

a) Axial mean velocity b) Axial rms velocity

Fig. 3 Axial mean and rms velocity predictions on the centerline.

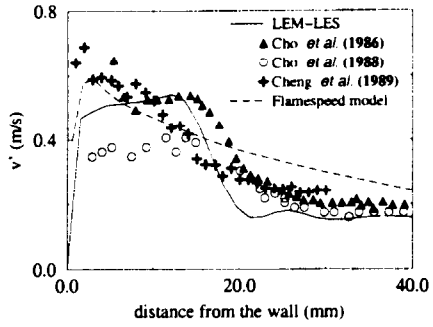

Fig. 4 Radial rms velocity predictions on the centerline.

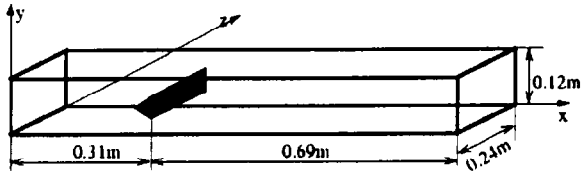

Fig. 5 Bluff-Body Configuration

a) case1 : Non-reacting flow

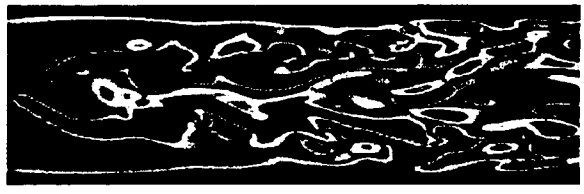

b) case2 : Reacting flow LES with the LEM

c) case3 : Reacting flow LES with a flame speed model

Fig. 6 Vorticity structure in the near wake of the bluff body. The contour corresponding to G = 0.5 is also shown for the reacting flow cases.

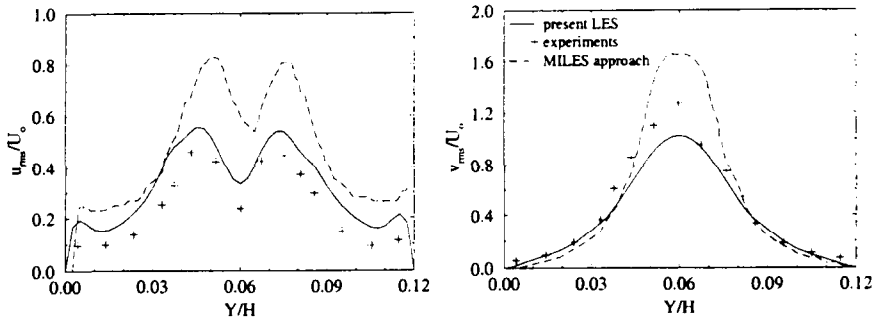

a) u_{rms} b) v_{rms}

Fig. 7 Intensity of velocity fluctuations at location 1 (x = 0.348 m) for the non-reacting case.

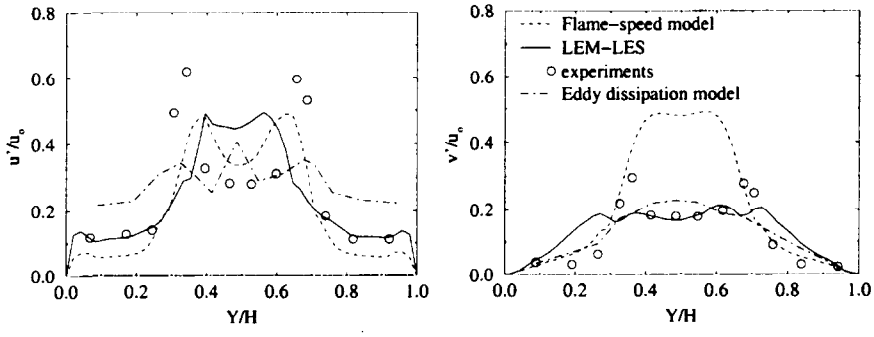

a) u_{rms} b) v_{rms}

Fig. 8 Intensity of velocity fluctuations at location 1 (x = 0.348 m) for the reacting case.

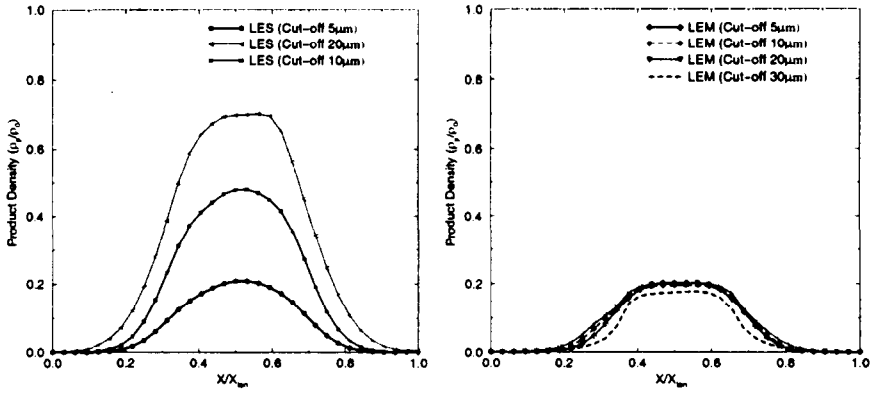

a) case1 : Conventional LES b) case2 : LES-LEM

Fig. 9 Product formation as predicted by different LES methods. The LES-LEM consistently predicts the same product formation even when the cutoff size is increased unlike the conventional LES.

a) $t = 0.0186$sec b) $t = 0.0238$sec

Fig. 10 Visualization of the highly swirling flow with droplet vaporization in a GE full-scale combustor. Figures show the vorticity magnitude in two axial planes and the product species mass fraction in the horizontal plan. The Reynolds number based in inlet diameter and velocity is 330,000 and swirl number is 0.56.

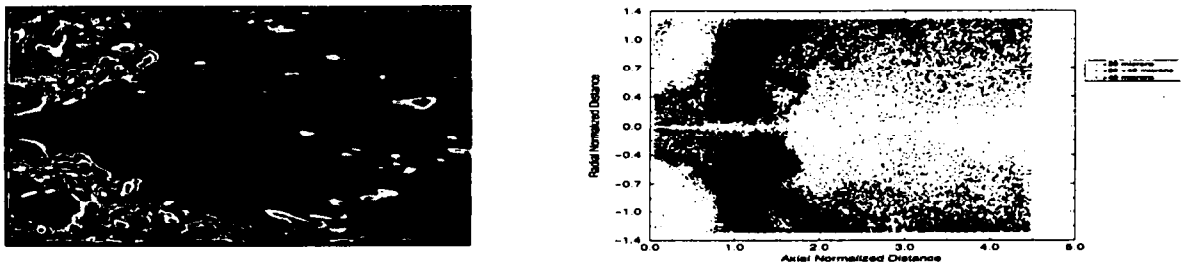

a) Vorticity magnitude in the center $x - y$ plane b) Droplet distribution in the center $x - y$ plane

Fig. 11 Center plane distribution of the vorticity and droplets in the GE full-scale combustor. The droplets spread out rapidly due to the high swirl in the flow with the smaller droplets traveling further from the vortex shear layer. However, note that vaporization is on going and therefore, large droplets are also rapidly becoming small.

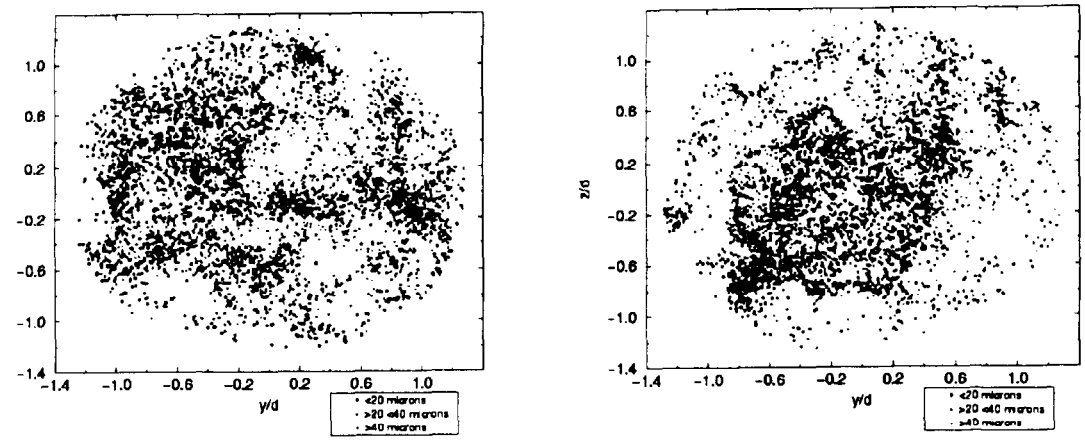

a) Droplet distribution at $t = 0.0186$sec

b) Droplet distribution at $t = 0.0238$sec

Fig. 12 Droplet distribution in the spanwise $y - z$ plane at $x/D = 1.13$.

a) Product density at $t = 0.0186$sec

b) Product density at $t = 0.0238$sec

Fig. 13 Product density distribution in the spanwise $y - z$ plane at $x/D = 1.13$.